Numer. Math. (2001) 90: 197–213
Digital Object Identifier (DOI) 10.1007/s002110100287

Numerische Mathematik

A posteriori error estimate and h-adaptive algorithm on surfaces for Symm's integral equation

C. Carstensen[1], **M. Maischak**[2], **E.P. Stephan**[2]

[1] Mathematical Seminar, University of Kiel, Ludwig-Meyn-Strasse 4, 24098 Kiel, Germany; e-mail: cc@numerik.uni-kiel.de
[2] Institute for Applied Mathematics, University of Hannover, Welfengarten 1, 30167 Hannover, Germany; e-mail: {maischak,stephan}@ifam.uni-hannover.de

Received November 29, 1999 / Revised version received August 10, 2000 /
Published online May 30, 2001 –

Summary. A residual-based a posteriori error estimate for boundary integral equations on surfaces is derived in this paper. A localisation argument involves a Lipschitz partition of unity such as nodal basis functions known from finite element methods. The abstract estimate does not use any property of the discrete solution, but simplifies for the Galerkin discretisation of Symm's integral equation if piecewise constants belong to the test space. The estimate suggests an isotropic adaptive algorithm for automatic mesh-refinement. An alternative motivation from a two-level error estimate is possible but then requires a saturation assumption. The efficiency of an anisotropic version is discussed and supported by numerical experiments.

Mathematics Subject Classification (1991): 65N38, 65N15, 65R20, 45L10

1 Introduction

The efficient numerical treatment of an integral equation of the first kind via an adaptive mesh-refining algorithm is studied in [2–8, 10, 14, 16, 18, 19] essentially for one-dimensional closed curves. Three-dimensional problems are considered in [5, 9, 13] and the theory therein will be complemented in this paper in the sense that we localise the estimate in [5], give different proofs and suggest different algorithms than in [9], and justify upper bounds of the estimate in [13] without any extra conditions such as the saturation assumption.

Correspondence to: C. Carstensen

To describe the main results, we consider Symm's integral equation which is equivalent to interior or exterior Dirichlet problems for the Laplacian in a bounded Lipschitz domain $\Omega \subset \mathbb{R}^3$ with boundary $\partial\Omega$ or on the open surface $\Gamma \subset \partial\Omega$: *Given f find ψ with*

$$V\psi(x) := \frac{1}{4\pi} \int_\Gamma \frac{\psi(y)}{|x-y|}\, ds_y = f(x) \quad (x \in \Gamma). \tag{1}$$

A Galerkin discretisation provides ψ_N and a partition $\mathcal{T} = \{\Gamma_1, \ldots, \Gamma_N\}$ of Γ in elements $\Gamma_1, \ldots, \Gamma_N$ with mesh-sizes $h_1, \ldots, h_N$ with the property that the residual R_N,

$$R_N(x) := f(x) - V\psi_N(x) \quad (x \in \Gamma), \tag{2}$$

satisfies a Poincaré inequality on Γ_j, i.e., there holds

$$\|R\|_{L^2(\Gamma_j)} \le C(\Gamma_j)\, |R|_{H^1(\Gamma_j)}. \tag{3}$$

Piecewise constant test functions cause $\int_{\Gamma_j} R_N\, ds = 0$ and so (3) with $C(\Gamma_j) \le \operatorname{diam}(\Gamma_j)$.

We will prove in Sect. 4 that (3) is sufficient for an a posteriori error estimate

$$\|\psi - \psi_N\|_{\tilde{H}^{-\alpha}(\Gamma)} \le c(\alpha, \mathcal{T}) \Big(\sum_{j=1}^N h_j^{2\alpha} \|\nabla R\|^2_{L^2(\Gamma_j)} \Big)^{1/2}, \tag{4}$$

where ∇ is the gradient on the 2D surface Γ, (and norms with $0 \le \alpha \le 1$ are described in Sect. 2). Since the upper bound consists of a sum of computable residuals $\eta_j := h_j^\alpha \|\nabla R\|_{L^2(\Gamma_j)}$, those serve as error indicators in an adaptive mesh-refining algorithm in Sect. 5. The underlying meshes are shape-regular as supposed in (4), but partly even more general.

The remaining part of this paper is organised as follows. The necessary notation and some preliminaries are recalled from the literature in Sect. 2. The main tool is the localisation by multiplication with hat-functions in Sect. 3 to prove abstract estimates which are applicable to any discretisation scheme or anisotropic meshes. In the aforementioned case of a Galerkin discretisation of Symm's integral equation (1), we prove (4) in Sect. 4 and discuss related questions. The motivated error indicators are compared and adaptive algorithms are presented in Sect. 5. Their efficient numerical performance is reported in Sect. 6 for a numerical example on an L-shaped open surface.

2 Preliminaries

Let Ω be a bounded Lipschitz domain in $\mathbb{R}^3$ with (closed) boundary $\partial\Omega$. Then, the norm in $H^1(\partial\Omega)$ is

$$\|v\|^2_{H^1(\partial\Omega)} = \|v\|^2_{L^2(\partial\Omega)} + \|\nabla v\|^2_{L^2(\partial\Omega)},$$

where ∇ denotes the gradient with respect to the arc-length along the two dimensional surface $\partial\Omega$. For $0 \le \alpha \le 1$, let $H^\alpha(\partial\Omega)$ be defined by (complex) interpolation of $H^1(\partial\Omega)$ and $L^2(\partial\Omega)$ (cf., e.g., [1]). The scalar product in $L^2(\partial\Omega) = H^0(\partial\Omega)$ extends to the duality pairing $\langle\cdot,\cdot\rangle$ in $H^\alpha(\partial\Omega)$ and $H^{-\alpha}(\partial\Omega)$,

$$H^\alpha(\partial\Omega) := (H^{-\alpha}(\partial\Omega))^* \qquad (\alpha < 0),$$

with $*$ denoting the dual space. We need two fractional Sobolev spaces $H^\alpha(\omega)$ and $\tilde{H}^\alpha(\omega)$ on arbitrary (relatively open) subset ω of $\partial\Omega$. If $[X_0, X_1]_s$ denotes (complex) interpolation of the Hilbert space X_0 and $X_1 \subset X_0$ for $0 \le s \le 1$, we define

$$H^s(\omega) := [L^2(\omega), H^1(\omega)]_s \quad \text{and} \quad \tilde{H}^s(\omega) := [L^2(\omega), H^1_0(\omega)]_s,$$

where $\tilde{H}^1(\omega) = H^1_0(\omega)$ denotes the closure of the test functions $C^\infty_0(\omega)$ with compact support in ω with respect to the $H^1(\omega)$-norm. For $-1 \le s \le 0$ we define

$$H^s(\omega) := (\tilde{H}^{-s}(\omega))^* \quad \text{and} \quad \tilde{H}^s(\omega) := (H^{-s}(\omega))^*.$$

The subsequent localisation property will be essential for the proofs below.

Lemma 2.1 ([8,17,15]) *Let $f_1, \ldots, f_n \in H^\alpha(\partial\Omega)$, $0 \le \alpha \le 1$, such that $f_j\, f_k = 0$ on $\partial\Omega$ whenever $1 \le j < k \le n$. Let $\omega_j :=$ interior$(\mathrm{supp} f_j)$ satisfy $\overline{\omega}_j = \mathrm{supp} f_j$. Then*

$$\Big\| \sum_{j=1}^n f_j \Big\|^2_{H^\alpha(\partial\Omega)} \le C_1 \sum_{j=1}^n \|f_j\|^2_{H^\alpha(\omega_j)}. \tag{5}$$

The constant C_1 depends on $\partial\Omega$ but does not depend on f_j or on n.

Remarks 2.1 (i) The lemma is proved by von Petersdorff in [17] and we have $C_1 = 1$ for complex interpolation in the sequel. The lemma is used by Stephan and Suri in [15] with $C_1 = C$ where $H^\alpha(\partial\Omega)$ is defined by real interpolation.
(ii) Faermann studied the assertion in [8] in case of real interpolation in two dimensions resp. the fractional Sobolev-Slobodeckij norm in three dimensions.

(iii) Recall that $H^\alpha(\partial\Omega)$ is equivalent to the trace space

$$H^\alpha(\partial\Omega) := \{v|_{\partial\Omega} \,:\, v \in H^{\alpha+1/2}(\mathbb{R}^3)\} \qquad (\alpha > 0)$$

of $H^{\alpha+1/2}(\mathbb{R}^3)$ with an equivalent trace norm [11]. (iv) Recall the interpolation estimate: For all $f \in H^1(\partial\Omega)$ and $0 \le \alpha \le 1$,

$$\|f\|_{H^\alpha(\partial\Omega)} \le C_2 \, \|f\|^{1-\alpha}_{L^2(\partial\Omega)} \, \|f\|^{\alpha}_{H^1(\partial\Omega)}. \tag{6}$$

We have $C_2 = 1$ for complex interpolation (also in case of sub-pieces).

3 Localisation

Lemma 2.1 separates the norms of functions with pairwise disjoint support. The techniques in [4] for their design are feasible on one-dimensional curves only. In this paper, we localise by multiplication with functions from a partition of unity with local supports.

Definition 3.1 *Let Ω be a bounded Lipschitz domain in $\mathbb{R}^3$. A finite partition of unity of $\partial\Omega$ is a finite sequence $\Phi := (\varphi_1, \ldots, \varphi_M)$ of Lipschitz functions $\varphi_1, \ldots, \varphi_M \,:\, \partial\Omega \to \mathbb{R}$ such that on $\partial\Omega$*

$$1 = \varphi_1 + \ldots + \varphi_M \text{ and } \varphi_1, \ldots, \varphi_M \ge 0. \tag{7}$$

Let the Lipschitz domain ω_j be the interior of suppφ_j *and suppose $\overline{\omega}_j =$* suppφ_j*. The overlap $K(\Phi)$ is defined by (*card$S$ *denotes the number of elements in a set S)*

$$K(\Phi) := \max_{j=1,\ldots,M} \text{card}\{k \in \{1,\ldots,M\} \,:\, \varphi_k \, \varphi_j \neq 0 \text{ on } \partial\Omega\}. \tag{8}$$

The point is that $K(\Phi)$ may be much smaller than M, even bounded, while M is increasing to infinity as the mesh-size tends to zero. Hence, we distribute $\varphi_1, \ldots, \varphi_M$ into a minimal number $\le K(\Phi)$ of groups to apply Lemma 2.1 in the proof of Theorem 3.1 below.

Lemma 3.1 *Let Φ be a finite partition of unity of $\partial\Omega$ with overlap $K(\Phi)$. Then there exists a partition of $\{1, \ldots, M\}$ into $K \le K(\Phi)$ non-empty subsets $M_1, \ldots, M_K$,*

$$\bigcup_{j=1}^{K} M_j = \{1, \ldots, M\} \text{ and}$$

$$M_j \cap M_k = \emptyset \text{ if } j \neq k \quad (j, k = 1, \ldots, K), \tag{9}$$

such that, for all $\ell \in \{1, \ldots, K\}$ and $j, k \in M_\ell$ with $j \neq k$,

$$\varphi_j \, \varphi_k = 0 \text{ on } \partial\Omega. \tag{10}$$

Proof. The index sets $M_1, \ldots, M_K$ are constructed by induction on $\mu = 1, 2, \ldots, K$ which stops for some $K \leq K(\Phi)$. To design M_1, fix φ_1 and set $M_{11} := \{1\}$. Given $M_{1\nu}$ we try to find $k \in \{1, \ldots, M\} \backslash M_{1\nu}$ with (10) for all $j \in M_{1\nu}$. If there is such a k we choose one (e.g., the smallest if there are more than one) and set $M_{1,\nu+1} := M_{1\nu} \cup \{k\}$. We repeat this procedure until we get some ν such that we find no k satisfying (10) for all $j \in M_{1,\nu}$. Then we define $M_1 := M_{1,\nu}$ and continue. (Note that M_1 is defined after a finite number of steps because $\{1, \ldots, M\}$ is finite.)

In this way we construct M_1 and assume now that we have constructed μ disjoint subsets $M_1, \ldots, M_\mu$ of $\{1, \ldots, M\}$. If $M_1 \cup \ldots \cup M_\mu = \{1, \ldots, M\}$ we stop and let $K := \mu$. Otherwise we select one entry k from $\{1, \ldots, M\} \backslash (\cup_{\kappa=1}^{\mu} M_\kappa) \neq \emptyset$ (e.g., its smallest element) and define $M_{\mu+1,1} := \{k\}$. Given $M_{\mu+1,\nu}$, we seek $k \in \{1, \ldots, M\} \backslash (M_{\mu+1,\nu} \cup \cup_{\kappa=1}^{\mu} M_\kappa)$ satisfying (10) for all $j \in M_{\mu+1,\nu}$. When we find such a k we set $M_{\mu+1,\nu+1} := M_{\mu+1,\nu} \cup \{k\}$. We repeat this procedure until we obtain some ν such that we find no k satisfying (10) for all $j \in M_{\mu+1,\nu}$. Then, we define $M_{\mu+1} := M_{\mu+1,\nu}$ and continue with $\mu + 1$. After a finite number of steps this construction will stop and yield a partition $M_1, \ldots, M_K$ of $\{1, \ldots, M\}$ which satisfies (10).

It remains to prove the bound of K. Consider $k \in M_K$. Then, $k \notin M_\mu$ for each $\mu \in \{1, \ldots, K-1\}$ and so (10) is not satisfied for at least one $j_\mu \in M_\mu$. Since $\varphi_k \, \varphi_{j_\mu} \neq 0$ for each $\mu \in \{1, \ldots, K-1\}$, there are at least $K-1$ functions amongst $\{\varphi_j : j = 1, \ldots, M; j \neq k\}$ whose supports have a non-void intersection with the support of φ_k. This proves $K \leq K(\Phi)$. □

Theorem 3.1 *Let Γ be a connected sub-piece of $\partial\Omega$ as in Sect. 2 and let Φ be a finite partition of unity of $\partial\Omega$ with overlap $K(\Phi)$. Then, for any $f \in H^\alpha(\partial\Omega)$ and $0 \leq \alpha \leq 1$, we have*

$$\|f\|^2_{H^\alpha(\Gamma)} \leq K(\Phi) \sum_{j=1}^{M} \|f \, \varphi_j\|^2_{H^\alpha(\omega_j)}. \tag{11}$$

Proof. By density, it is enough to prove the assertion for a Lipschitz function f. We consider a partition $M_1, \ldots, M_K$ of $\{1, \ldots, M\}$ as in Lemma 3.1. According to (7), $f = \sum_{j=1}^{M} \varphi_j \, f$ and we obtain

$$\begin{aligned} \|f\|^2_{H^\alpha(\Gamma)} \leq \|f\|^2_{H^\alpha(\partial\Omega)} &= \Big\| \sum_{j=1}^{M} \varphi_j \, f \Big\|^2_{H^\alpha(\partial\Omega)} \\ &= \Big\| \sum_{k=1}^{K} \sum_{j \in M_k} \varphi_j \, f \Big\|^2_{H^\alpha(\partial\Omega)} \leq K \sum_{k=1}^{K} \Big\| \sum_{j \in M_k} \varphi_j \, f \Big\|^2_{H^\alpha(\partial\Omega)}, \end{aligned}$$

where we use that $(\sum_{j=1}^n a_j)^2 \le n(\sum_{j=1}^n a_j^2)$. Next we apply Lemma 2.1 to $\{f\,\varphi_j : j \in M_k\}$ and infer

$$\Big\| \sum_{j\in M_k} \varphi_j\, f\Big\|^2_{H^\alpha(\partial\Omega)} \le \sum_{j\in M_k} \|\varphi_j\, f\|^2_{H^\alpha(\omega_j)}.$$

Using this in the above estimate we deduce

$$\|f\|^2_{H^\alpha(\Gamma)} \le K \sum_{k=1}^K \sum_{j\in M_k} \|\varphi_j\, f\|^2_{H^\alpha(\omega_j)} = K \sum_{j=1}^M \|\varphi_j\, f\|^2_{H^\alpha(\omega_j)}. \qquad \square$$

We need some notation to define the geometry in the abstract estimate below.

Definition 3.2 *The width* $\mathrm{width}(\omega)$ *of* $\omega \subset \partial\Omega$ *is the smallest number* $d \ge 0$ *such that the following is true. There exists* $d > 0$ *and some direction* $n \in \mathbb{R}^3$, $|n| = 1$, *such that, for each* $x \in \mathbb{R}^3$ *and for each plane* $H(x,n) := \{y = x + m \in \mathbb{R}^3 : m \cdot n = 0\}$ *through* x *perpendicular to* n, $\omega \cap H(x,n)$ *is a Lipschitz curve of arc-length* $\le d$. *If there exists no such* n, *let* $\mathrm{width}(\omega) := \infty$.

Theorem 3.2 *Let* Φ *be a finite partition of unity on* $\partial\Omega$ *with overlap* $K(\Phi)$ *and let* ω_j *the interior of* $\mathrm{supp}\varphi_j$ *and* $d_j := \mathrm{width}(\omega_j)$ *for each* $j \in \{1,\dots,M\}$. *Then, for* $0 < \alpha < 1$, $\Gamma \subset \partial\Omega$, *and* $f \in H^1(\partial\Omega)$, *we have*

$$\|f\|^2_{H^\alpha(\Gamma)} \le K(\Phi) \sum_{j=1}^M d_j^{2(1-\alpha)}\,(1+d_j^2)^\alpha\, \|\nabla(\varphi_j\, f)\|^2_{L^2(\omega_j)}. \tag{12}$$

Proof. By Theorem 3.1 and according to the interpolation estimate (6) we obtain

$$\|f\|^2_{H^\alpha(\Gamma)} \le K(\Phi) \sum_{j=1}^M \|f\,\varphi_j\|^{2(1-\alpha)}_{L^2(\partial\Omega)}\, \|f\,\varphi_j\|^{2\alpha}_{H^1(\partial\Omega)}. \tag{13}$$

Finally, Friedrichs' inequality yields (even with a smaller constant)

$$\|f\,\varphi_j\|^{2(1-\alpha)}_{L^2(\partial\Omega)}\, \|f\,\varphi_j\|^{2\alpha}_{H^1(\partial\Omega)} \le d_j^{2(1-\alpha)}\,(1+d_j^2)^\alpha\, \|\nabla(\varphi_j\, f)\|^2_{L^2(\omega_j)}. \qquad \square$$

We conclude this section with a modification of a recent result [8,9] obtained so far by direct calculations with Sobolev-Slobodeckij norms.

Theorem 3.3 *Let Φ be a finite partition of unity on $\partial\Omega$ with overlap $K(\Phi)$ and let $0 \le \alpha \le 1$ and $\Gamma \subset \partial\Omega$. Suppose that $f \in H^1(\partial\Omega)$ satisfies $\int_{\omega_j} f\,ds = 0$ for all $j = 1, \ldots, M$. Then we have*

$$\|f\|^2_{H^\alpha(\Gamma)} \le C \sum_{j=1}^{M} \|f\|^2_{H^\alpha(\omega_j)}. \tag{14}$$

The constant $C > 0$ in (14) depends on Γ, $\partial\Omega$, $K(\Phi)$, $d_j \operatorname{Lip}(\varphi_j)$, and the shape (but neither size nor number) of the patches ω_j.

Proof. The proof will follow from interpolation of the operator ($|\omega_j|$ denotes the area of ω_j and j is fixed in $\{1, \ldots, M\}$)

$$T_s : H^s(\partial\Omega) \to H^s(\omega_j), \quad f \mapsto \varphi_j(f - \int_{\omega_j} f\,ds/|\omega_j|).$$

It is obvious that T_0 is bounded with an operator norm ≤ 1. For $s = 1$ we argue as in the proof of Theorem 3.2 (this time with Poincaré's inequality) and deduce

$$\begin{aligned}
&\left\| \nabla \left(\varphi_j \left(f - \int_{\omega_j} f\,ds/|\omega_j| \right) \right) \right\|_{L^2(\omega_j)} \\
&\quad \le \left\| \left(f - \int_{\omega_j} f\,ds/|\omega_j| \right) \nabla\varphi_j \right\|_{L^2(\omega_j)} + \|\varphi_j\,\nabla f\|_{L^2(\omega_j)} \\
&\quad \le \operatorname{Lip}(\varphi_j) \left\| f - \int_{\omega_j} f\,ds/|\omega_j| \right\|_{L^2(\omega_j)} + \|\nabla f\|_{L^2(\omega_j)} \\
&\quad \le (1 + \operatorname{Lip}(\varphi_j) C(\omega_j))\ \|\nabla f\|_{L^2(\omega_j)}.
\end{aligned}$$

This shows that T_1 is bounded with an operator norm $\le C$. Then, interpolation theory shows that T_α is bounded as well [1]. This and Theorem 3.1 prove the assertion. □

Remarks 3.1 The estimate (14) is shown in [8, 9] for Sobolev-Slobodeckij norms. Then, without any restrictions on the mesh, the converse inequality to (14) is true. We refer to [8, 9] for details.

4 Symm's integral equation

Let Ω be a bounded polyhedron with boundary $\partial\Omega$ with (open) faces and let $\Gamma \subset \partial\Omega$ with a Lipschitz curve $\partial\Gamma$. Given $f \in H^1(\Gamma)$ we seek $\psi \in$

$\tilde{H}^{-1/2}(\Gamma)$ satisfying (1) with the linear, bounded and bijective single-layer potential operator $V : \tilde{H}^{\alpha-1}(\Gamma) \to H^{\alpha}(\Gamma)$ (defined in (1)) for $0 < \alpha < 1$.

In the first case let $\psi_N \in L^2(\Gamma)$ denote an arbitrary approximation to the unique solution ψ with a residual $R_N := f - V\psi_N$. It is stressed that no assumption relates R_N and the Lipschitz partition of unity $\varphi_1, \ldots, \varphi_M$. Recall that the patch ω_j is the interior of $\mathrm{supp}(\varphi_j) = \overline{\omega}_j$ and let $\delta_j := \mathrm{diam}(\omega_j)$ denote its diameter.

Corollary 4.1 *There exists a constant $C > 0$ that depends only on $0 < \alpha < 1$, Γ, and $\partial\Omega$ such that for any $\psi_N \in L^2(\Gamma)$ and $R_N := f - V\psi_N$ we have*

$$\|\Psi - \Psi_N\|^2_{\tilde{H}^{-\alpha}(\Gamma)} \le C \sum_{j=1}^{N} \delta_j^{2\alpha} \|\nabla(\varphi_j R_N)\|^2_{L^2(\omega_j)}. \tag{15}$$

Proof. The proof follows from $\psi - \psi_N = V^{-1}R_N$, the boundedness of V^{-1}, and Theorem 3.2. □

In the second case let $\psi_N \in L^2(\Gamma)$ denote some approximation such that the residual $R_N := f - V\psi_N$ has an integral $\int_{\Gamma_k} R_N \, ds = 0$ over each element Γ_k with diameter h_k of a partition $\mathcal{T} = \{\Gamma_1, \ldots, \Gamma_N\}$ of Γ as in the introduction. Suppose that the supports of hat functions φ_j are matched exactly by a finite number of elements. Then, the Galerkin condition $\int_{\Gamma_k} R_N \, ds = 0$ (for all $k = 1, \ldots, N$) implies $\int_{\omega_j} R_N \, ds = 0$ (for all $j = 1, \ldots, M$).

Corollary 4.2 *There exists a constant $C > 0$ that depends only on $0 < \alpha < 1$, Γ, $\partial\Omega$, and the shape (not the size) of the elements and patches such that for any $\psi_N \in L^2(\Gamma)$ and $R_N := f - V\psi_N$ with $\int_{\omega_j} R_N \, ds = 0$ for all $j = 1, \ldots, M$, we have*

$$\|\Psi - \Psi_N\|^2_{\tilde{H}^{-\alpha}(\Gamma)} \le C \sum_{j=1}^{N} h_j^{2\alpha} \|\nabla R_N\|^2_{L^2(\Gamma_j)}. \tag{16}$$

Proof. The proof follows from the previous Corollary plus a Poincaré inequality which shows (cf. (3))

$$\|R_N\|^2_{L^2(\omega_j)} \le C(\omega_j) \|\nabla R_N\|^2_{L^2(\omega_j)}$$

and so verifies (recall $0 \le \varphi_j \le 1$ and $\mathrm{Lip}(\varphi_j)\, C(\omega_j) \le C$ for a locally uniform mesh)

$$\begin{aligned} \|\nabla(\varphi_j R_N)\|^2_{L^2(\omega_j)} &\le \|R_N \, \nabla\varphi_j\|^2_{L^2(\omega_j)} + \|\varphi_j \, \nabla R_N\|^2_{L^2(\omega_j)} \\ &\le \mathrm{Lip}(\varphi_j) \|R_N\|^2_{L^2(\omega_j)} + \|\nabla R_N\|^2_{L^2(\omega_j)} \\ &\le C \|\nabla R_N\|^2_{L^2(\omega_j)}. \end{aligned}$$

□

The following corollary is shown in [8,9] for Sobolev-Slobodeckij norms and assumes the same conditions as Corollary (4.2) in the second case.

Corollary 4.3 *There exists a constant $C > 0$ that depends only on $0 < \alpha < 1$, Γ, $\partial\Omega$, and the shape (not the size) of the elements such that for any $\psi_N \in L^2(\Gamma)$ and $R_N := f - V\psi_N$ with $\int_{\omega_j} R_N\, ds = 0$ for all $j = 1, \ldots, M$, we have*

$$\|\Psi - \Psi_N\|^2_{\tilde{H}^{-\alpha}(\Gamma)} \leq C \sum_{j=1}^{M} \|R_N\|^2_{H^\alpha(\omega_j)}. \tag{17}$$

Proof. The proof follows from Theorem 3.3 if we argue as before. □

Remarks 4.1 (i) It is emphasised that Corollary 4.1 is valid for *any* approximation obtained on *any* mesh (or even with a mesh-less method) without any shape-regularity.
(ii) Corollary 4.2 motivates the isotropic error indicator

$$\mu_j := h_j^{1/2} \|\nabla R_N\|_{L^2(\Gamma_j)} \tag{18}$$

since $C(\sum_{j=1}^N \mu_j^2)^{1/2}$ is a computable upper error bound with respect to the energy norm.
(iii) Open surfaces yield edge singularities near the edge which limit the regularity of the exact solution ψ, in general, $\psi \notin L^2(\Gamma)$. It is well-established that edge singularities require anisotropic elements and in our numerical experiments below, the aspect ratio of rectangles is increasing. In those situations, an anisotropic error indicator such as

$$\mu_{j,k} := h_{j,k}^{1/2} \|\partial R_N / \partial x_k\|_{L^2(\Gamma_j)} \quad (k = 1, 2) \tag{19}$$

is expected to reflect the singular behaviour in a more appropriate way than (18). In (19), Γ_j is an axes-parallel rectangle with edge-lengthes $h_{j,1}$ and $h_{j,2}$.
(iv) The authors failed to prove that $C(\sum_{j=1}^N (\mu_{j,1}^2 + \mu_{j,2}^2))^{1/2}$ is an upper error bound.
(v) Corollary 4.3 motivates the (rather theoretical) error indicator

$$\nu_j := \|R_N\|_{H^\alpha(\omega_j)}, \tag{20}$$

where the norm in $H^\alpha(\omega_j)$ is to be evaluated for complex interpolation. Besides the interpolation estimate (6) the authors do not know of another upper bound that is easy to compute.

Instead, Faermann first proves that Theorem 3.3 is true when replacing the complex interpolated norm by the Sobolev-Slobodeckij norm [9] and then suggests to evaluate the local Sobolev-Slobodeckij norm in (20) with an

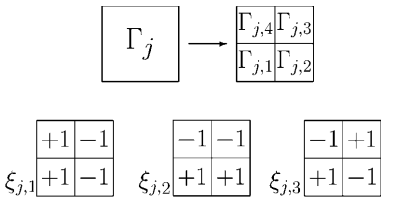

Fig. 1. Refinement of Γ_j into four new elements and the basis functions $\xi_{j,1}, \xi_{j,2}, \xi_{j,3}$

accurate quadrature rule. The striking advantage of her approach is efficiency for arbitrary meshes (cf. Remark 3.1).
(vi) A two-level ansatz and a saturation assumption are used in [13] to see, for quasi-uniform meshes, that, up to multiplicative constants, $(\sum_{j=1}^N(\eta_{j,1}^2+\eta_{j,2}^2+\eta_{j,3}^2))^{1/2}$ is a lower and upper error bound, where

$$\eta_{j,k} := \frac{\langle R_N, \xi_{j,k}\rangle}{\langle V\xi_{j,k}, \xi_{j,k}\rangle^{1/2}} \quad (k=1,2,3) \tag{21}$$

and the ansatz functions $\xi_{j,k}$ are defined for one rectangle by dividing it into four congruent rectangles in Fig. 1.
(vii) Another interpretation for (21) and a motivation for the decision for an anisotropic mesh-refinement along either the x_1- or the x_2-axis is possible by a line search in the direction $\xi_{j,k}$, i.e., a separate energy minimisation along the one-dimensional affine space $\psi_N + \mathbb{R}\,\xi_{j,k}$. Direct calculations for the energy $E(\varphi) = \frac{1}{2}\langle V\varphi, \varphi\rangle - \langle f, \varphi\rangle$ show

$$\min_{s\in\mathbb{R}} E(\psi_N + s\,\xi_{j,k}) = -\frac{\langle R_N, \xi_{j,k}\rangle^2}{\langle V\xi_{j,k}, \xi_{j,k}\rangle} - \frac{1}{2}\langle V\psi_N, \psi_N\rangle,$$

which, up to a ψ_N-dependent additive constant, equals $-\eta_{j,k}^2$. Hence, motivated by a minimal energy in a separate line search, we prefer a refinement along the x_k-axes for that k that maximises the term $\eta_{j,k}$ amongst $k=1$ or $k=2$.
(viii) The question of efficiency of the a posteriori error estimate (16) remains open in general. Arguing as in [3] one could prove that $(\sum_{j=1}^N \mu_j^2)^{1/2}$ is, up to a multiplicative constant and higher order terms, a lower bound of the error as well. The severe assumptions for this are a quasi-uniform mesh (to guarantee inverse estimates and asymptotic convergence properties) and a closed boundary (to ensure $\psi \in L^2(\Gamma)$).

5 Error indicators and adaptive algorithms

The error indicators μ_j, $\mu_{j,k}$, ν_j, and $\eta_{j,k}$ in (18)-(21) from the a posteriori error estimates of the previous section can be ordered and employed for steering automatic mesh-refinements.

Theorem 5.1 *There exist constants $c_1, c_2, c_3 > 0$ which depend on the aspect ratio of the elements $\Gamma_1, \ldots, \Gamma_N$ in $\mathcal{T}$ and on Γ, Ω but not on f, $R_N := f - V\psi_N$, or $\psi = V^{-1}f$ and neither on the sizes nor numbers of elements in $\mathcal{T}$ such that we have*

$$\eta_{j,k} \le c_1 \mu_{j,k} \le c_1 \mu_j \qquad (k = 1, 2;\ j = 1, \ldots, N), \tag{22}$$

$$\left(\sum_{\Gamma_\ell \subset \overline{\omega}_j} \left(\eta_{1,\ell}^2 + \eta_{2,\ell}^2 \right) \right)^{1/2} \le c_2\, \nu_j \le c_3 \left(\sum_{\Gamma_\ell \subset \overline{\omega}_j} \mu_\ell^2 \right)^{1/2} \tag{23}$$
$$(j = 1, \ldots, M).$$

(The inequalities that involve $\eta_{j,k}$ require $\alpha = 1/2$ while the other inequalities are valid for all α.)

Proof. The function $\xi_{j,k}$ can be written as the derivative of a hat-function $\phi_{j,k}$ with height $h_{j,k}/2$. Integration by parts and Cauchy's inequality show

$$\langle R_N, \xi_{j,k} \rangle = -\langle \partial_{x_k} R_N, \phi_{j,k} \rangle \le \|\phi_{j,k}\|_{L^2(\Gamma_j)} \|\partial_{x_k} R_N\|_{L^2(\Gamma_j)}. \tag{24}$$

The function $\xi_{j,1}$ can be also written as the difference of two characteristic functions $\xi_{j,1} = \chi_1 - \chi_2$ (see Fig. 1). χ_1 and χ_2 are rectangles with side lengths $h_{j,1}/2$ and $h_{j,2}$. From

$$\begin{aligned} V(\chi_1 - \chi_2, \chi_1 - \chi_2) &= V(\chi_1, \chi_1) + V(\chi_2, \chi_2) - 2V(\chi_1, \chi_2) \\ &= 2V(\chi_1, \chi_1) - 2V(\chi_1, \chi_2) \end{aligned}$$

and the following formulae (obtained with direct integration)

$$\begin{aligned} &4\pi\, V(\chi_1, \chi_1) \\ &\quad = \frac{2}{3}\left(h_{j,1}/2\right)^3 + \frac{2}{3} h_{j,2}^3 - \frac{1}{6}((h_{j,1}/2)^2 + h_{j,2}^2)^{3/2} \\ &\qquad + \frac{h_{j,1} h_{j,2}}{2} \left(\frac{h_{j,1}}{2} \mathrm{arsinh}\left(\frac{2h_{j,2}}{h_{j,1}} \right) + h_{j,2} \mathrm{arsinh}\left(\frac{h_{j,1}}{2h_{j,2}} \right) \right), \\ &4\pi\, V(\chi_1, \chi_2) \\ &\quad = 2(h_{j,1}/2)^3 - \frac{1}{3} h_{j,2}^3 + \frac{2}{3}((h_{j,1}/2)^2 + h_{j,2}^2)^{3/2} - \frac{1}{3}(h_{j,1}^2 + h_{j,2}^2)^{3/2} \\ &\qquad - 2h_{j,1} h_{j,2} \left(\frac{h_{j,1}}{2} \mathrm{arsinh}\left(\frac{2h_{j,2}}{h_{j,1}} \right) + h_{j,2} \mathrm{arsinh}\left(\frac{h_{j,1}}{2h_{j,2}} \right) \right) \\ &\qquad + 2h_{j,1} h_{j,2} \left(h_{j,1} \mathrm{arsinh}\left(\frac{h_{j,2}}{h_{j,1}} \right) + h_{j,2} \mathrm{arsinh}\left(\frac{h_{j,1}}{h_{j,2}} \right) \right), \end{aligned}$$

we eventually deduce that (writing $h_{j,3} := h_{j,1}$)

$$
\begin{aligned}
&2\pi\langle V\xi_{j,k},\xi_{j,k}\rangle\\
&\quad= -\frac{h_{j,k}^3}{6} + h_{j,k+1}^3 - \frac{1}{6}(h_{j,k}^2+4h_{j,k+1}^2)^{3/2} + \frac{1}{3}(h_{j,1}^2+h_{j,2}^2)^{3/2}\\
&\qquad +4h_{j,1}h_{j,2}\left(\frac{h_{j,k}}{2}\mathrm{arsinh}\left(\frac{2h_{j,k+1}}{h_{j,k}}\right)+h_{j,k+1}\mathrm{arsinh}\left(\frac{h_{j,k}}{2h_{j,k+1}}\right)\right)\\
&\qquad -2h_{j,1}h_{j,2}\left(h_{j,k}\mathrm{arsinh}\left(\frac{h_{j,k+1}}{h_{j,k}}\right)+h_{j,k+1}\mathrm{arsinh}\left(\frac{h_{j,k}}{h_{j,k+1}}\right)\right).
\end{aligned}
$$

Inspection of the last term shows that it is indeed equivalent to $h_{j,k}|\Gamma_j|$. Using this and equivalence of $\|\phi_{j,k}\|_{L^2(\Gamma_j)}$ to $h_{j,k}(|\Gamma_j|)^{1/2}$ we deduce from (24) that

$$
\frac{\langle R_N,\xi_{j,k}\rangle}{\langle V\xi_{j,k},\xi_{j,k}\rangle^{1/2}} \le c_1\frac{\|\phi_{j,k}\|_{L^2(\Gamma_j)}}{(h_{j,k}|\Gamma_j|)^{1/2}}\|\partial_{x_k}R_N\|_{L^2(\Gamma_j)} \le c_1\mu_{j,k}.
$$

This proves the first estimate in (22), the second is obvious.

To verify (23), recall that in (20), $H^\alpha(\Gamma_j)$ is defined by complex interpolation and so, with $C_2=1$ in (6), we deduce

$$
\nu_j \le \|R_N\|_{L^2(\omega_j)}^{1-\alpha}\|R_N\|_{H^1(\omega_j)}^{\alpha}.
$$

This and Poincaré's inequality $\|R_N\|_{L^2(\omega_j)} \le C(\omega_j)\|\nabla R_N\|_{L^2(\omega_j)}$ conclude the proof of the second inequality in (23). To prove the first inequality by complex interpolation, define

$$
T_\alpha : H^\alpha(\omega_j)\to\mathbb{R},\quad f\mapsto\langle f,\xi_{\ell,k}\rangle.
$$

It is obvious that the operator norm of T_0 is bounded $\|\xi_{\ell,k}\|_{L^2(\Gamma_\ell)}$. For $s=1$ we notice that $\xi_{\ell,k}$ has integral mean zero and so, with the integral mean $\bar f$ of f over Γ_ℓ, we have

$$
|T_1 f| = |\langle f,\xi_{\ell,k}\rangle| = |\langle f-\bar f,\xi_{\ell,k}\rangle|.
$$

A Cauchy and a Poincaré inequality guarantee

$$
|T_1 f| \le \|f-\bar f\|_{L^2(\Gamma_\ell)}\|\xi_{\ell,k}\|_{L^2(\Gamma_\ell)} \le C(\Gamma_\ell)\|f\|_{H^1(\omega_j)}\|\xi_{\ell,k}\|_{L^2(\Gamma_\ell)}.
$$

Interpolation of the two bounds for T_α for $\alpha=0,1$ shows

$$
|\langle f,\xi_{\ell,k}\rangle| \le \|T_\alpha\|\,\|f\|_{H^\alpha(\omega_j)} \le C(\Gamma_\ell)^\alpha\,\|\xi_{\ell,k}\|_{L^2(\Gamma_\ell)}\,\|f\|_{H^\alpha(\omega_j)}.
$$

This estimate and the above computation of $\langle V\xi_{\ell,k},\xi_{\ell,k}\rangle$ verify the first inequality in (23) (since the sum is finite). □

The numerical experiments reported in Sect. 6 are run with the three algorithms (A)–(C) which differ in the use of the error indicator and the refinement procedure in step (4). Therein, $0\le\Theta\le 1$ is a parameter for uniform ($\Theta=0$) or adaptive mesh-generation.

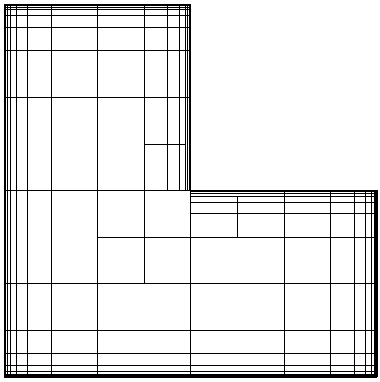

Fig. 2. Mesh $\mathcal{T}_{10}$ generated by Algorithm (B)

Algorithm (A), (B), (C) (i) Start with an intimal mesh $\mathcal{T}_0$ and set $m = 0$.
(ii) Compute Galerkin solution ψ_N for current mesh $\mathcal{T}_m = \{\Gamma_1, \ldots, \Gamma_N\}$.
(iii) Compute error indicators indicators μ_j, $\mu_{j,k}$, and $\eta_{j,k}$ from (18)-(21).
(iv) For Algorithm (A), refine Γ_j into four congruent rectangles provided

$$\mu_j \geq \Theta \max\{\mu_1, \ldots, \mu_N\}.$$

For Algorithm (B), halve Γ_j along the x_k-axis for $k = 1$ and $k = 2$ provided

$$\mu_{j,k} \geq \Theta \max\{\mu_{1,k}, \ldots, \mu_{N,k}\}.$$

For Algorithm (C), halve Γ_j along the x_k-axis for $k = 1$ and $k = 2$ provided

$$\eta_{j,k} \geq \Theta \max\{\eta_{1,k}, \ldots, \eta_{N,k}\}.$$

(v) Generate the new mesh $\mathcal{T}_{m+1}$ according to (4) and update m. Stop or go to (ii).

6 Numerical example

The algorithms (A), (B), and (C) were run to solve Symm's integral equation (1) with a right-hand side $f = 1$ and an initial mesh $\mathcal{T}_0$ that contained 12 congruent squares to cover the L-Shape Γ. The computations were performed using the program *maiprogs* [12]. The error indicators $\mu_j, \mu_{j,k}$ were approximated by numerical integration of the analytical computed gradient of the residual by a 4×4-Gaussian quadrature rule, while $\eta_{j,k}$ was calculated exactly using the algorithms of the computation of the Galerkin matrix.

Algorithm (B) generated a sequence of meshes $(\mathcal{T}_m)_{m=1,2,3,\ldots}$ for $\Theta = 0.5$. The meshes $\mathcal{T}_{10}$, $\mathcal{T}_{15}$, resp. $\mathcal{T}_{20}$ are plotted in Fig. 2, 3, resp. 4. We observe strong anisotropic refinements parallel and towards all edges which reflects expected edge-singularities.

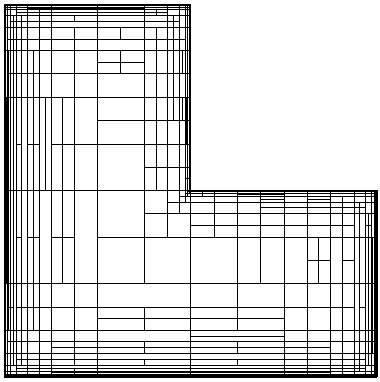

Fig. 3. Mesh $\mathcal{T}_{15}$ generated by Algorithm (B)

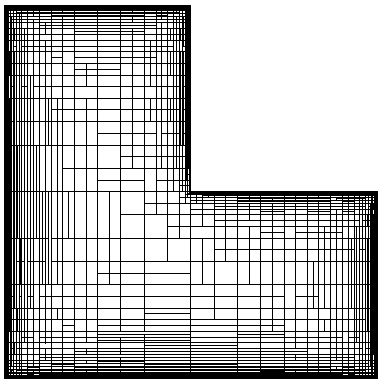

Fig. 4. Mesh $\mathcal{T}_{20}$ generated by Algorithm (B)

The energy norm of the solution Ψ of $V\psi = 1$ is known to be $\langle V\psi, \psi\rangle^{1/2} = 2.878293$ and this is employed to compute the energy error norms through

$$e_N^2 := \langle V(\psi - \psi_N), \psi - \psi_N\rangle = \langle V\psi_N, \psi_N\rangle - \langle V\psi, \psi\rangle$$

(by Galerkin-orthogonality). Table 1 gives the results for the meshes generated by Algorithm (B) where N is the degree of freedoms, e_N is the error in the energy norm, and $\eta_N = (\sum_{j=1}^{N} \mu_j^2)^{1/2}$ is the computed upper error bound (for $\alpha = 1/2$ without taking the constant factor into account). The experimental convergence rate α_N is computed as

$$\alpha_N = \frac{\log(e_{N'}/e_N)}{\log(N/N')}, \tag{25}$$

where N' and $e_{N'}$ are the corresponding values of the previous row. The convergence rates observed in Table 1 are much higher than $1/4$ (expected for a uniform mesh-refinement) and so indicate an efficient mesh-refining. The

Table 1. Error indicators and efficiency for $\theta = 0.5$

N	η_N	e_N	e_N/η_N	α_N
12	0.9558277	0.6646427	1.438108	
33	0.7157455	0.4917142	1.455613	0.29789
64	0.5231094	0.3603837	1.451534	0.46911
105	0.3791923	0.2621146	1.446666	0.64310
148	0.2857298	0.1968658	1.451394	0.83396
184	0.2220168	0.1548582	1.433678	1.10237
245	0.1641732	0.1158337	1.417319	1.01408
306	0.1275614	0.0909866	1.401980	1.08598
371	0.0984725	0.0707287	1.392257	1.30757
450	0.0789983	0.0579766	1.362589	1.02987
540	0.0638628	0.0465304	1.372496	1.20629
656	0.0509174	0.0376706	1.351647	1.08548
805	0.0411453	0.0308533	1.333580	0.97535
968	0.0340271	0.0260617	1.305636	0.91532
1243	0.0266476	0.0207189	1.286148	0.91749
1543	0.0217106	0.0173712	1.249805	0.81513
1902	0.0179114	0.0144254	1.241652	0.88835
2418	0.0145247	0.0118803	1.222581	0.80867
3127	0.0116897	0.0097656	1.197027	0.76231
3926	0.0096766	0.0081669	1.184856	0.78566

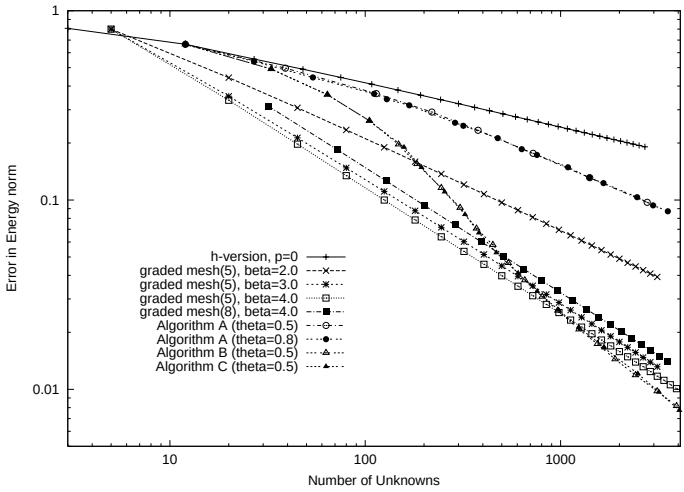

Fig. 5. Dirichlet problem on the L-shape in $\mathbb{R}^3$

quotients e_N/η_N stay about 1.1 till 1.5 which indicates a reasonable overall error estimation (although the bound of V^{-1} is not included in Table 1).

To report on several related experiments in a more compact form, we plotted the entries (N, e_N) for varies numbers of N from the output of Algorithm (A), (B), (C), resp. a sequence of graded meshes $(\mathcal{T}_m)_{m=0,1,2,\ldots}$ in

one diagram where the horizontal N- and the vertical e_N-axis are scaled logarithmically. Related entries are plotted with the same symbol (e.g., $\circ, +, \times$) and linked by (e.g., full, dashed, dotted) straight lines in Fig. 5. We refer to the legend for further details and conclude this section with a few observations from Fig. 5 and similar experiments.

Remarks 6.1 (i) For uniform and graded meshes, the superiority of a grading with a parameter $(j/J)^4$ for $j = 0, \ldots, J$ gives the best results (overgrading leads to larger condition numbers without sufficient improvement).
(ii) Algorithm (A) is not competitive, there is a need for anisotropic mesh-refinement.
(iii) The change of the parameter Θ (in the range $0.5 \leq \Theta \leq 1$) does not necessarily improve the meshes.
(iv) Algorithm (B) and (C) yield very similar results and can compete for higher degrees of freedom with optimally graded meshes.

Acknowledgements. It is our pleasure to thank the German Research Foundation (DFG) and the Australian Research Council (ARC) for support through the DFG-ARC German-Australian Collaboration in Numerical Analysis of Boundary Integral Methods and Applications in Sydney in September 1999 where parts of this paper were finalised. The first author thanks Birgit Faermann for several remarks on some technical details that led to an improved and clearer presentation of the results.

References

1. J. Bergh, J. Löfström: Interpolation Spaces, vol. 223 of Grundlehren der mathematischen Wissenschaften, Berlin: Springer 1976
2. C. Carstensen: Adaptive boundary element methods and adaptive finite element and boundary element coupling, in Boundary Value Problems and Integral Equations on Non Smooth Domains, M. Costable, M. Dauge, and S. Nicaise, eds., vol. 167 of Lecture notes in pure and applied mathematics, pp.47–58. New York: Marcel Dekker 1995
3. C. Carstensen: Efficiency of a posteriori bem error estimates for first kind integral equations on quasi-uniform meshes. Math. Comp. **65**, 69—84 (1996)
4. C. Carstensen: An a posteriori error estimate for a first kind integral equation. Math. Comp. **66**, 139–155 (1997)
5. C. Carstensen, E. P. Stephan: A posteriori error estimates for boundary element methods. Math. Comp. **64**, 483–500 (1995)
6. C. Carstensen, E. P. Stephan: Adaptive boundary element method for some first kind integral equations. SIAM J. Numer. Analysis **32**, 2166–2183 (1996)
7. B. Faermann: Local a posteriori error indicators for the galerkin discretisation of boundary integral equations. Numer. Math. **79**, 43–76 (1998)
8. B. Faermann: Localization of the Aronszajn-Slobodeckij norm and application to adaptive boundary element methods. Part I. The two-dimensional case. IMA J. Numer. Anal. **20**, 203–234 (2000)

9. B. Faermann: Localization of the Aronszajn-Slobodeckij norm and application to adaptive boundary element methods. Part II. The three-dimensional case, Numer. Math. (2001) (accepted)
10. N. Heuer: hp-Versionen der Randelementmethode. PhD thesis, Universität Hannover, 1992
11. J. Lions, E. Magenes: Non-Homogeneous Boundary Value Problems and Applications I. Berlin: Springer 1972
12. M. Maischak: Manual of the program system maiprogs, preprint, Institut für Angewandte Mathematik, Universität Hannover, 1999
13. P. Mund, E. P. Stephan, J. Weiße: Two-level methods for the single layer potential in $\mathbb{R}^3$. Computing **60**, 243–266 (1998)
14. E. Rank: Adaptive boundary element methods, in Boundary Elements IX, C.A Brebbia, W.L. Wendland, G. Kuhn (eds.) vol. 1, pp. 259–278. Heidelberg: Springer 1987
15. E. P. Stephan, M. Suri: The h-p version of the boundary element method on polygonal domains with quasiuniform meshes. RAIRO Analy. Numer. **25**, (6) 783–807 (1991)
16. E. P. Stephan, W. L. Wendland: Remarks to Galerkin and least squares methods with finite elements for general elliptic problems. Manuscripta Geodaetica **1**, 93–123 (1976)
17. T. von Petersdorff: Randwertprobleme der Elastizitätstheorie für Polyeder – Singularitäten und Approximation mit Randelementmethoden. PhD thesis, Darmstadt, 1989
18. W. L. Wendland, De-hao Yu: Adaptive boundary element methods for strongly elliptic integral equations. Numer. Math. **53**, 539–558 (1988)
19. W. L. Wendland, De-hao Yu: A posteriori local error estimates of boundary element methods with some pseudo-differential equations on closed curves. Journal for Computational Mathematics **10**, 273–289 (1992)